# The transcription factor Cdx2 regulates inflammasome activity through expression of the NLRP3 suppressor TRIM31 to maintain intestinal homeostasis

Sanzida Jahan[1], Nidaa Awaja[1], Bradley Hess[1], Stephanie Hajjar[2], Subash Sad[2], and David Lohnes[1],*

From the [1]Department of Cellular and Molecular Medicine, and [2]Department of Biochemistry, Microbiology, and Immunology, University of Ottawa, Ottawa, Ontario, Canada

Edited by Peter Cresswell

The intestine-specific transcription factor Cdx2 is essential for intestinal homeostasis and has been implicated in the pathogenesis of disorders including inflammatory bowel disease. However, the mechanism by which Cdx2 influences intestinal disease is not clear. Here, we present evidence supporting a novel Cdx2–TRIM31–NLRP3 (NLR family, pyrin domain containing 3) signaling pathway, which may represent a mechanistic means by which Cdx2 impacts intestinal inflammation. We found that conditional loss of Cdx function resulted in an increase in proinflammatory cytokines, including tumor necrosis factor alpha, interleukin (IL)-1β, and IL-6, in the mouse colon. We further show that *TRIM31*, which encodes a suppressor of NLRP3 (a central component of the NLRP3 inflammasome complex) is a novel Cdx2 target gene and is attenuated in the colon of Cdx conditional mutants. Consistent with this, we found that attenuation of *TRIM31* in Cdx mutant intestine occurs concomitant with elevated levels of NLRP3 and an increase in inflammasome products. We demonstrate that specific inhibition of NLRP3 activity significantly reduced IL-1β and IL-6 levels and extended the life span of Cdx conditional mutants, reflecting the therapeutic potential of targeting NLRP3. Tumor necrosis factor-alpha levels were also induced independent of NLRP3, potentially *via* elevated activity of the proinflammatory NF-κB signaling pathway in Cdx mutants. Finally, *in silico* analysis of ulcerative colitis patients revealed attenuation of CDX2 and TRIM31 expression coincident with enhanced expression of proinflammatory cytokines. We conclude that the novel Cdx2–TRIM31–NLRP3 signaling pathway promotes proinflammatory cytokine expression, and its inhibition may have therapeutic potential in human intestinal diseases.

Inflammatory bowel disease (IBD) is characterized by a noninfectious, chronic, and relapsing intestinal inflammation. IBD includes Crohn's disease, ulcerative colitis (UC), and indeterminate colitis (1). Given the long-term morbidity, rising incidence, and increased susceptibility to colorectal cancer in those with IBD, it is vital to better understand the molecular mechanisms underlying these disorders. In the absence of such advances, management of IBD is expected to remain suboptimal despite the availability of potential therapeutic options (2).

Although the etiology of IBD is not fully understood, it is generally believed to result from a dysbiosis, where an inappropriate immune response is evoked in reaction to environmental cues, such as commensal microbes (3). IBD has also been linked to a variety of genetic polymorphisms (4), and genome-wide association studies and candidate gene analyses have provided compelling evidence that IBD represents a class of polygenic disorders, with over 240 susceptibility loci reported to date (5, 6).

Inflammasomes are multiprotein complexes that regulate the maturation and activation of proinflammatory caspases (7). The NLRP3 (NLR family, pyrin domain containing 3) inflammasome is a regulator of innate immunity (8, 9). Upon activation, the NLRP3 inflammasome triggers proteolytic maturation of the cysteine protease caspase-1, which subsequently cleaves and activates the cytokines interleukin (IL)-1β and IL-18 (10). Unrestricted NLRP3 activation can lead to chronic inflammation resulting in mucosal damage and thus can play a role in IBD (11–13), prompting the use of NLRP3 inflammasome inhibitors as a potential therapeutic option for certain cases of IBD (14). While activation of the NLRP3 inflammasome needs to be tightly regulated to maintain homeostasis in the intestine (15, 16), the mechanisms governing the expression of NLRP3, and their role in inflammation and homeostasis, are incompletely understood (10).

The intestinal epithelium is a continually self-renewing tissue, and the proper execution of differentiation programs is critical for intestinal homeostasis (17). Cdx1 and Cdx2 homeodomain proteins are intestinal transcription factors that regulate intestinal epithelial differentiation and are essential for gut homeostasis (18, 19). Cdx members elicit their effects by direct binding to target loci at Cdx response elements (CDREs) to increase or decrease target gene transcription, at least in part, by alterations in chromatin architecture (20, 21).

Cdx2 dysfunction has been implicated in the pathogenesis of IBD (22), and several IBD susceptibility genes, such as *HNF4α, Meprin 1A (MEP1A), Peptide transporter 1, CLDN2,*

*Laminin subunit γ2 (LAMC2)*, and *Mucin 2* are regulated by Cdx2 (22–25). Moreover, Boyd *et al.* (26) identified genomic regions of CDX2 occupancy in Caco-2 cells and recovered a number of IBD-associated genes as potential direct CDX targets, including *TCF7L2*, *LGALS8*, *Cd9*, and *Mep1A* (24, 27–29). These findings underscore the prospective involvement of CDX2 in the pathogenesis of IBD, although the mechanisms remain poorly understood. In this regard, although *Cdx2* null mice are early lethal, *Cdx2* heterozygous offspring are sensitized to dextran sodium sulfate–induced colitis (30), consistent with a protective role for Cdx in IBD. The clinical relevance of this relationship is further evidenced by the attenuation of expression of *CDX2* in UC patients and its re-expression following leukocytapheresis in responsive individuals (31). Moreover, increased levels of tumor necrosis factor alpha (TNF-α), a cytokine central to the proinflammatory events in IBD, correlate with attenuated *CDX2* expression in UC patients, and TNF-α can likewise suppress *CDX2* expression in model systems (23). These observations contribute to a growing body of evidence supporting a role for CDX2 in IBD.

*Cdx1* and *Cdx2* are coexpressed in the murine intestinal epithelium, where they functionally overlap (19, 32, 33). Moreover, *Cdx2* homozygous null mutants are periimplantation lethal (34). To circumvent this functional overlap and early lethality, we created a *Cdx2* "floxed" conditional allele and crossed this into a *Cdx1* null mutant background. We then assessed the impact of the loss of all *Cdx* functions in the intestine, using a tamoxifen-regulated Villin-CreER[T] transgene to delete *Cdx2*. Using this approach, we previously demonstrated that Cdx2, and to a lesser extent Cdx1, is required for intestinal homeostasis and that Cdx members function as tumor suppressors in an adenomatous polyposis coli model of colorectal cancer (21, 35–40).

In the present study, we found that loss of *Cdx* function led to induction of a proinflammatory cascade in colon epithelium, including elevated NLRP3 protein and accumulation of products of the NLRP3 inflammasome. We further found that *TRIM31*, which encodes a negative regulator of the NLRP3 inflammasome (41, 42), is directly regulated by Cdx2, offering a mechanistic basis for these observations. The physiological relevance of this relationship is underscored by the finding that chemical inhibition of NLRP3 activity decreased levels of IL-1β and IL-6 induced by Cdx loss and lengthened the life span of *Cdx* conditional mutants. We also observed increased expression of *NF-κb2* and *Rela*, suggesting a basis for the elevated levels of TNF-α in *Cdx* mutants. Finally, *in silico* analysis revealed a strong inverse correlation between *CDX2*, *TRIM31*, and the levels of proinflammatory markers, including products of the NLRP3 inflammasome, in UC patients, underscoring the potential clinical relevance of these findings.

## Results

### Cdx deletion leads to intestinal inflammation

We generated *Cdx1*^{−/−}–*Cdx2*[fl]/[fl]-*Villin*-Cre ER[T] conditional mutant mice and treated them with tamoxifen to induce *Cdx2* deletion, yielding mice lacking *Cdx1* and *Cdx2* throughout the intestinal epithelium (termed *Cdx*-DKO hereafter; DKO [double KO]) as previously described (Fig. S1A) (35). Three days post-treatment, mice developed diarrhea, lethargy, rapid weight loss, and other indices of intestinal insufficiency and necessitating endpointing at 6-day post-treatment. Histological analysis revealed pathological alterations in intestinal epithelium as previously reported (35) (Fig. S1B).

Colon epithelial cells were isolated from WT and *Cdx*-DKO mice 6 days following treatment with tamoxifen and used for transcriptome profiling by RNA-Seq. This analysis revealed 6442 genes that were differentially expressed at a padj/false discovery rate of 0.05, with approximately equal numbers of genes upregulated (3231) and downregulated (3211) in the *Cdx*-DKO colon compared with controls (Fig. 1A). Kyoto Encyclopedia of Genes and Genomes functional enrichment analysis revealed a marked upregulation of genes involved in cytokine signaling, particularly the TNF-α pathway (Fig. 1B).

Additional bioinformatics analysis was performed for the top 500 differentially expressed genes. For each replicate, normalized counts were plotted, and data bars were added to the side to show the mean level of expression and log2Fold-Change for each gene. A list of all genes downloaded from Ensembl was annotated with the Gene Ontology (GO) term "Inflammatory response" (GO: 0006954) comprising a total of 759 genes. Any gene in the heatmap that is annotated with this term was flagged with a *red bar*. In colon epithelium from *Cdx*-DKO mice, 19 proinflammatory genes were upregulated, whereas 13 genes were downregulated (Fig. 1C).

### Cdx deficiency promotes the expression of proinflammatory cytokines

Genes encoding a number of cytokines and chemokines were induced in the Cdx DKO intestine, including *TNF-α*, *IL-1β*, *CXCL1*, and *CCL2*, as determined by RNA-Seq analyses and confirmed by RT–quantitative PCR (qPCR) (Figs. 2, *A–E* and S2, *A–D*). We were also able to detect upregulation of IL-6, which is a downstream target of IL-1β (43), by ELISA (Fig. 2F).

IL-1β is activated by the NLRP3 inflammasome, prompting us to examine the consequence of Cdx deletion on the expression of the components of this pathway. We found that the protein levels of NLRP3, pro-caspase-1, caspase-1, IL-1β, and IL-18 were all significantly elevated in Cdx mutants compared with WT (Figs. 3, *A–G* and S6).

Inflammatory cytokines secreted by the intestinal epithelium have a functional role in recruiting cells of the innate immune system. We therefore used flow cytometry to compare the levels of infiltrating monocytes (Ly6C-hi:Ly6G-low) and neutrophils (Ly6C-hi:Ly6G-hi) in the colons of *Cdx*-DKO and WT mice and found a significant increase in both types of immune cells in the mutant samples (Fig. 3, *H–J*).

### Identification of Cdx target genes

To better understand the means by which Cdx function impacts intestinal inflammation, we conducted chromatin immunoprecipitation followed by deep sequencing (ChIP-Seq)
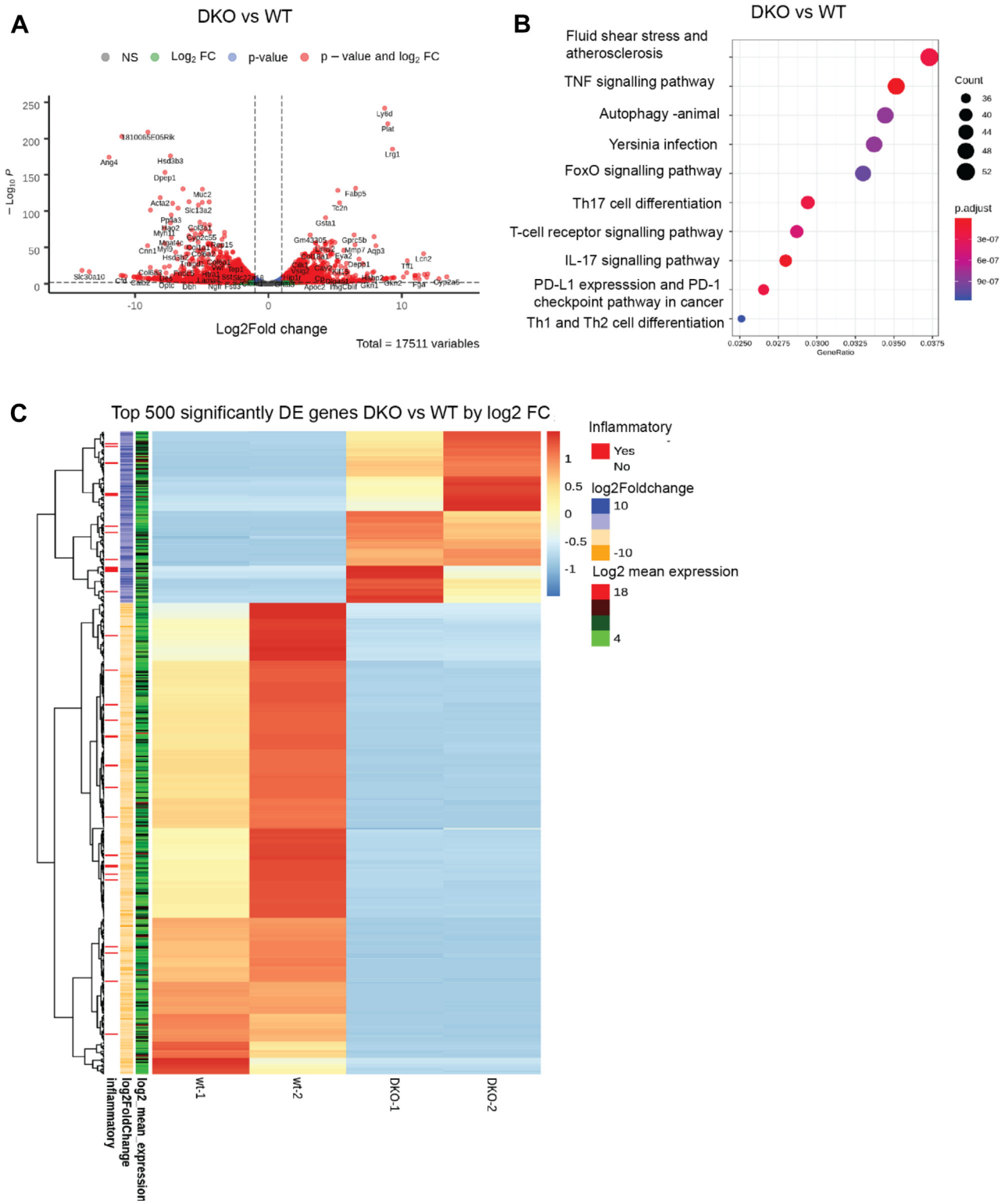
**Figure 1. Cdx deletion leads to inflammation.** *A*, volcano plot analysis of differentially expressed (DE) genes from RNA-Seq analysis comparing Cdx DKO *versus* WT colon epithelium. *B*, KEGG functional enrichment analysis for DE genes reveals induction of *TNF-α* and other inflammation-related pathways in the mutant epithelium. *C*, heatmaps of the top 500 DE genes. Bars at the side are scaled to indicate the mean level of expression and the log2FoldChange for each gene. Genes annotated with the term "Inflammatory response" (GO: 0006954), or any child term in the ontology, are denoted with a *red bar*. DKO, double KO; GO, Gene Ontology; KEGG, Kyoto Encyclopedia of Genes and Genomes; TNF-α, tumor necrosis factor alpha.

using chromatin prepared from colon epithelial cells and a Cdx2 antibody as described previously (19, 44). Approximately 5100 sites were identified using MACS2 peak calling annotated to genes that have Cdx2 bound in the region from −20 kb to +5kb relative to the transcriptional start site (TSS). Genomic distribution analysis revealed that these peaks were
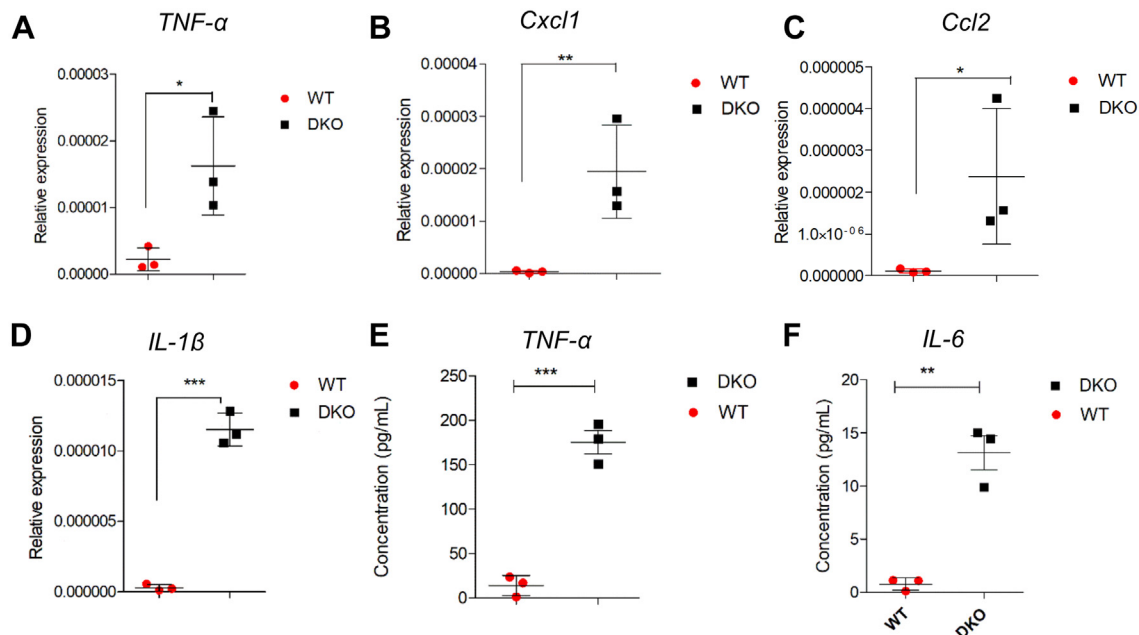
**Figure 2. Inflammatory cytokines are induced in Cdx mutants.** RT–qPCR quantification of relative expression for (*A*) *IL-1β*; (*B*) *TNF-α*; (*C*) *Cxcl1*; and (*D*) *Ccl2*. Expression was normalized using18s rRNA. *E* and *F*, ELISA for (*E*) TNF-α and (*F*) IL-6 from WT and Cdx DKO colon epithelium. Error bars represent the standard deviation from the mean of three independent biological experiments. Statistical significance was calculated using two-tailed *t* test, *$p < 0.05$, **$p < 0.01$, and ***$p < 0.001$. DKO, double KO; *IL-1β*, interleukin 1β; qPCR, quantitative PCR; *TNF-α*, tumor necrosis factor alpha.

primarily localized in intergenic (35.1%) and intronic (37.7%) regions, followed by proximal promoter (≤1 kb from the TSS; 13%) and upstream promoter (1–3 kb; 8.8%) regions (Fig. S3*A*). Analysis of sequences under the ChIP-Seq peaks revealed significant enrichment for the motif TTTATGGCT, consistent with previous observations for the consensus CDRE (Fig. S3*B*) (44–50).

ChIP-Seq for H3K4me3 was also performed as a surrogate measure of active transcription. In addition, as Cdx has been shown to impact gene expression *via* chromatin remodeling (20, 21), ATAC-Seq was also conducted to examine the impact of Cdx status on chromatin accessibility. ATAC-Seq and ChIP-Seq profiles for all protein-coding genes from Ensembl were created using the mouse reference genome UCSC mm10. The signal was normalized to counts per million, and the Cdx2 binding profile shown on a distinct color scale (range, 0–0.2 for Cdx2, 0–0.5 for ATAC-Seq and H3K4me3). Genes were examined for significant differential expression in Cdx mutants (Up_in_KO, Down_in_KO) or not differentially expressed (NC_in_KO). Heatmap analyses showed chromatin accessibility (ATAC-Seq) in control cells aligning with Cdx2 peaks and H3K4me3. Markedly lower signals were observed for ATAC-Seq in a subset of genes that were downregulated in DKO mutants as determined by RNA-Seq, suggesting Cdx impacts the expression of these genes *via* altered chromatin accessibility (Fig. 4*A*).

### TRIM31 *is a direct Cdx target gene*

To further identify potential direct Cdx target genes implicated in intestinal inflammation, we intersected Cdx2 occupancy as well as altered genome accessibility and differential expression (>1.4-fold altered expression). This yielded a list of

227 genes that were bound by Cdx2, exhibited altered chromatin accessibility, and were differentially expressed in *Cdx* mutant colon (Fig. 4*B*). *TRIM31* was recovered from among these genes.

Examination of the *TRIM31* locus revealed a major Cdx2 binding peak within the promoter region (Fig. 4*C*) with occupancy confirmed by ChIP–PCR (Fig. S5*A*). Alignment of the ATAC-Seq tracks between WT and Cdx mutant samples revealed Cdx-dependent loss of accessibility in mutant cells (Fig. 4*C*), which correlated with attenuation of *TRIM31* expression (Fig. 4*D*). Cdx-dependent regulation of *TRIM31* was also validated by RT–qPCR and immunoblot analysis from both mouse colon epithelium (Fig. 4, *E–G*) and *Cdx* conditional mutant colon organoid cultures (Fig. S4). In addition, Cdx2 occupancy, chromatin accessibility, and expression correlated with loss of the active chromatin mark H3K4me3 at the promoter region of *TRIM31* following Cdx deletion (Fig. S5*B*). Finally, we identified a putative CDRE under the ChIP-Seq peak, comprised of the sequence TTTATG (Fig. 4*H*).

To further assess Cdx-dependent regulation of *TRIM31*, we employed heterologous reporter assays using *TRIM31* promoter sequences containing either a WT or a mutated CDRE driving expression of a luciferase reporter gene. This analysis revealed that expression of the WT reporter was Cdx dependent in C2bbe1 intestinal cells, and that this response required the CDRE (Fig. 4*I*). Taken together, these findings strongly suggest that *TRIM31* is a direct Cdx target gene in the intestinal epithelium.

### NLRP3-dependent intestinal inflammation in Cdx mutant mice

*TRIM31* encodes a ubiquitin E3 ligase and has previously been identified as a suppressor of the NLRP3 inflammasome
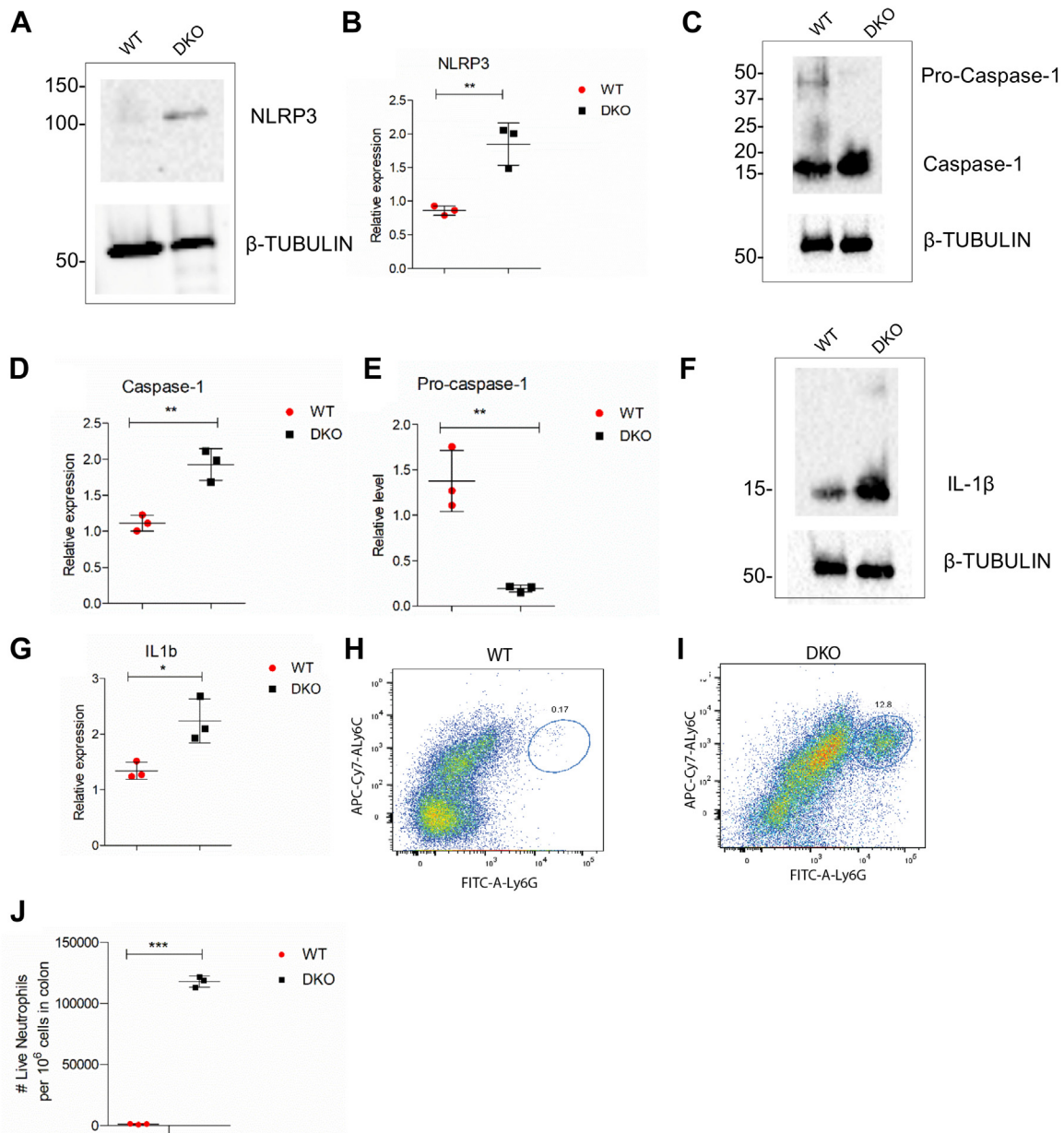
**Figure 3. The NLRP3 inflammasome is induced in Cdx mutants.** *A–G*, immunoblot analyses for (*A* and *B*) NLRP3; (*C–E*) caspase-1; and (*F* and *G*) IL-1β. The lower molecular weight bands for the latter two immunoblots represent the processed forms of the proteins. *H–J*, flow cytometric dot plots of freshly isolated primary intestinal cells for Ly6C- and Ly6G-positive cells (indicated by *circles* in *H* and *I*) obtained from WT (*H*) and DKO (*I*) colon and quantified in (*J*). Living cells were selected based on the absence of Zombie yellow staining. Cell sorting was based on the expression of either EpCAM or CD45 in the double-stained samples. Cells were gated based on size and granularity using FSC-A *versus* SSC-A to eliminate debris and clumped cells. Error bars represent the standard deviation from the mean of three independent biological experiments. Statistical significance was calculated using two-tailed *t* test, *$p < 0.05$, **$p < 0.01$, and ***$p < 0.001$. DKO, double KO; FSC-A, forward scatter area; IL-1β, interleukin 1β; NLRP3, NLR family, pyrin domain containing 3; SSC-A, side scatter area.

(42). This raises the possibility that Cdx-dependent intestinal inflammation could be due, at least in part, to attenuated expression of TRIM31 and subsequent induction of the NLRP3 inflammasome, as observed in Cdx-DKO mice (Fig. 3).

To further examine this relationship, we assessed the effect of inhibiting the NLRP3 inflammasome with a specific antagonist, CY-09 (51). To this end, WT or Cdx conditional mutant mice were treated with CY-09 or saline for 2 days, followed by tamoxifen treatment and continuation of CY-09 (or saline) treatment (Fig. 5A). Mice were euthanized on day 5 post-tamoxifen or when moribund, and the expression of the

proinflammatory cytokines TNF-α, IL-1β, and IL-6 measured by ELISA from colon extracts. In addition, NLRP3 was examined by immunofluorescence (IF), and IL-18 expression and processing assessed by immunoblot from colon epithelial cells after depletion of CD-45-positive immune cells.

When compared with saline-treated conditional mutant mice, CY-09-treated *Cdx*-DKO mice survived longer (Fig. 5B), suggesting that the NLRP3-mediated inflammatory response contributes to their demise. Notably, CY-09 had no inhibitory effect on the baseline levels of inflammatory markers in WT mice, whereas it reduced IL-1β and IL-6 in *Cdx* mutants, with
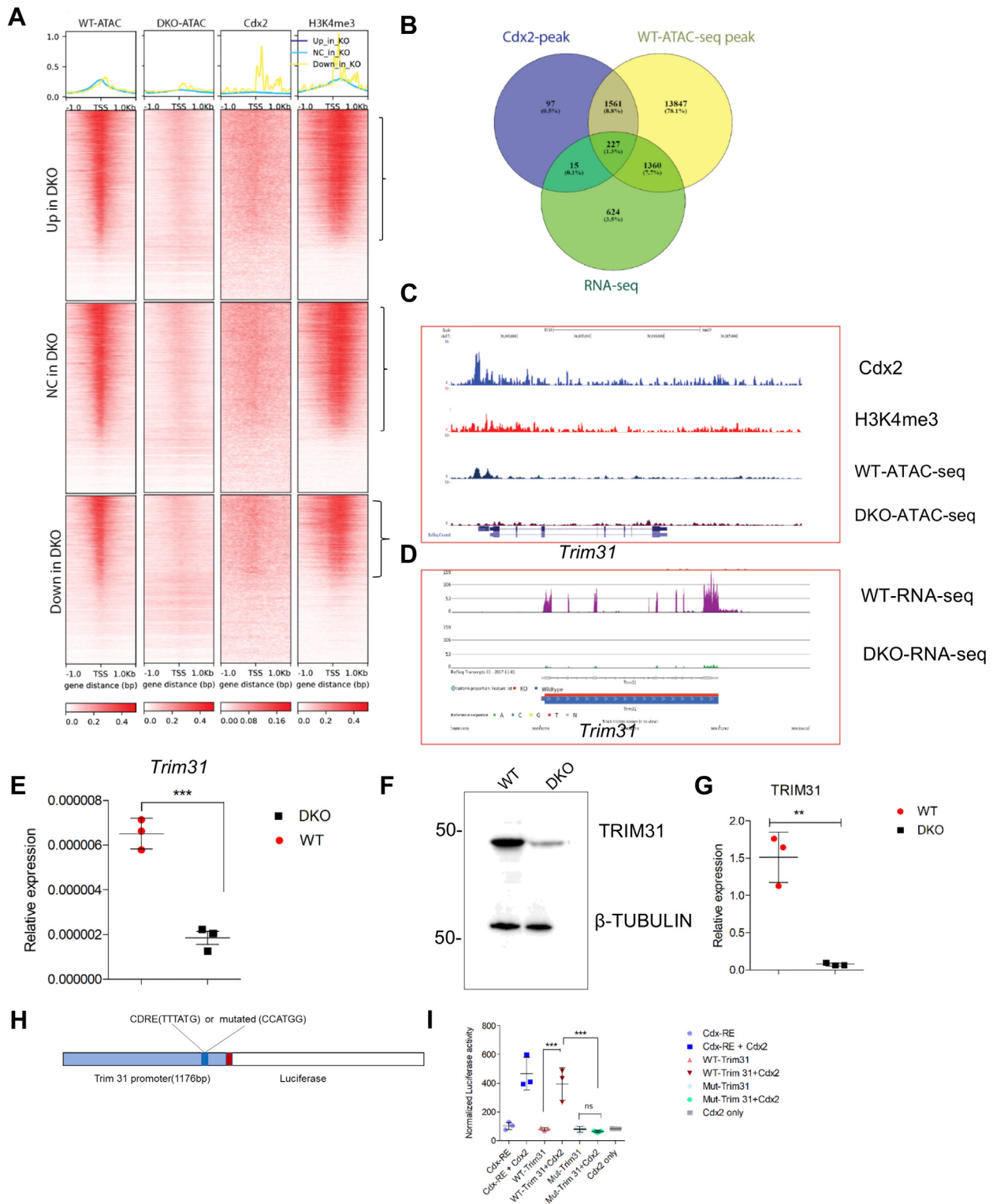
**Figure 4. *TRIM31* is a Cdx target gene.** *A*, ATAC-Seq and ChIP-Seq profiles were plotted for all protein-coding loci from Ensembl. The signal was normalized to counts per million, and the profiles were plotted relative to the genomic transcription start sites. Genes were divided according to whether they were significantly upregulated or downregulated in the DKO (Up_in_DKO, Down_in_DKO) or were not significantly changed (NC_in_DKO). *B*, common overlapping peaks among Cdx2 ChIP-Seq, ATAC-Seq, and downregulated genes from RNA-Seq revealed 227 candidate direct target genes. *C*, snapshot of Cdx2 binding and ATAC-Seq peak from WT and DKO colon epithelium showing Cdx2 occupancy of the *TRIM-31* locus and attenuation of chromatin accessibility in the DKO cells at *TRIM31*. *D*, RNA-Seq track showing attenuation of *TRIM31* expression in the DKO mutant colon. *E*, RT-qPCR quantification of relative expression changes for *TRIM31* confirming attenuation in Cdx mutant colon cells. *F*, immunoblot analysis of TRIM31 showing loss of protein in the DKO colon epithelium and (*G*) quantification of TRIM31 expression from three biological replicates. *H*, *TRIM31* promoter region used for heterologous reporter assays denoting the WT and mutant CDRE. *I*, heterologous reporter assays in C2BBE1 cells. Note the loss of responsiveness in the Mut-*TRIM31* reporter. Cdx-RE is a positive-control reporter for Cdx response. Error bars represent the standard error of the mean from three independent biological experiments. ****p* < 0.001. ChIP, chromatin immunoprecipitation; DKO; double KO; qPCR, quantitative PCR.
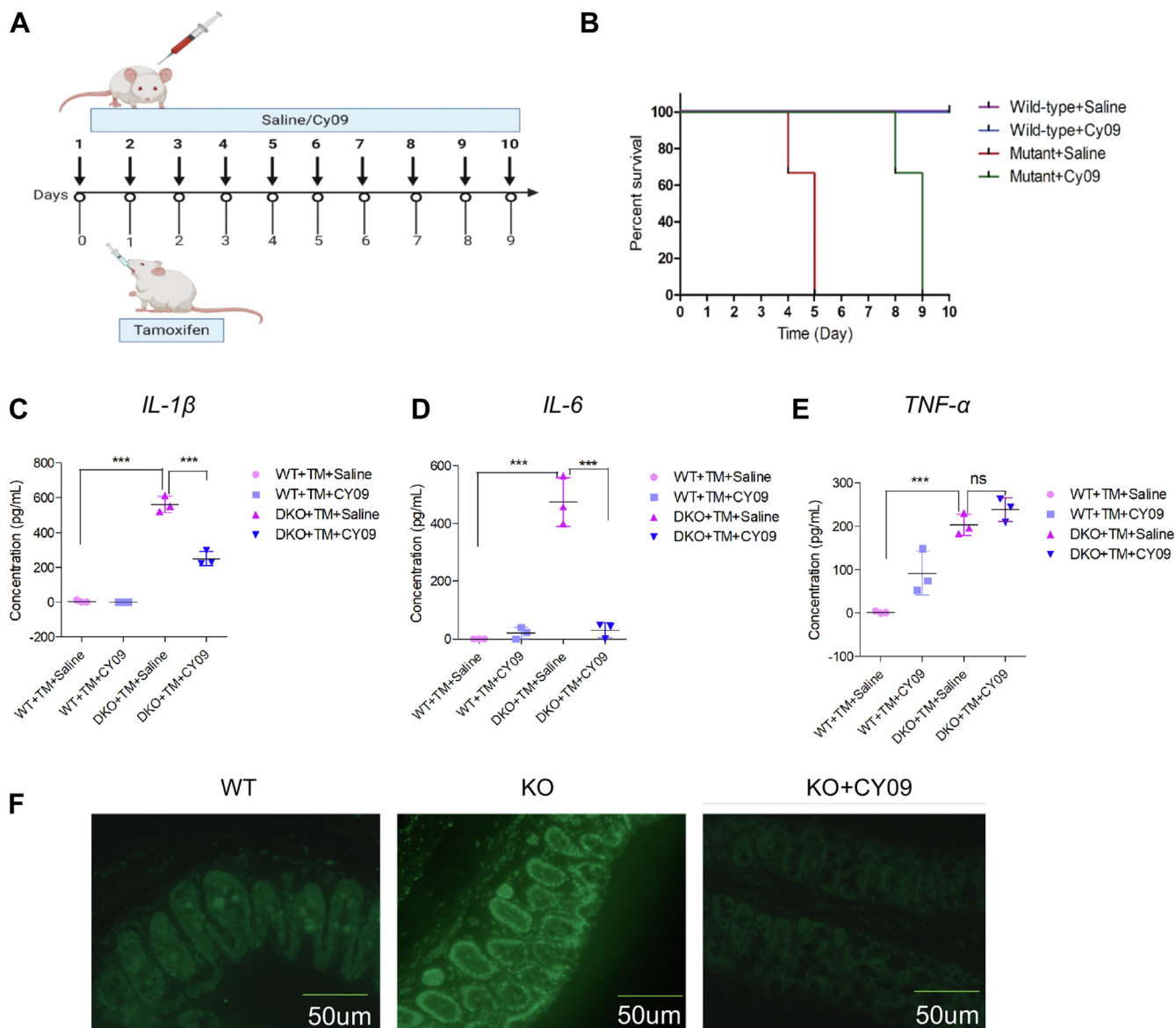
**Figure 5. NLRP3-dependent inflammation in Cdx mutant colon.** *A*, WT or mutant mice were treated daily with either the NLRP3 inhibitor CY-09 or saline. Mice were tamoxifen induced on day 2, treatment with CY-09 or saline continued, and animals were monitored for 6 days or until moribund. *B*, a Kaplan–Meier survival curve for each treatment group. A comparison of the curves reveals a *p* value of 0.0027 for vehicle *versus* inhibitor-treated DKO mutants. *C–E*, ELISA analysis for (*C*) IL-1β, (*D*) IL-6, and (*E*) TNF-α. Statistical significance was calculated using two-tailed *t* test and one-way ANOVA. ***$p < 0.001$. *F*, immunofluorescence for NLRP3 from colon sections of WT, Cdx DKO mutants, and CY-09-treated mice. DKO, double KO; IL, interleukin; NLRP3, NLRP3, NLR family, pyrin domain containing 3; ns; not significant; TNF-α, tumor necrosis factor alpha.

TNF-α remaining unchanged (Fig. 5, *C–E*). CY-09 did not affect the levels of *IL-1β* or *IL-6* transcripts (Fig. S7, *A* and *B*), consistent with the inhibitor acting post-transcriptionally. The epithelial nature of this effect is consistent with IF analysis, which revealed that an induction of NLRP3 was observed in the epithelial cells of the mutant colon, and that this expression was reduced by CY-09 treatment (Fig. 5*F*). In addition, IL-18 protein expression and activation was observed in immune-purified mutant colon epithelial cells (Fig. S6).

### NF-κB expression in Cdx mutants

The activation and nuclear translocation of NF-κB transcription factors is a crucial step for the transcription of a number of proinflammatory genes, including *TNF-α*. TNF-α receptor activation can further enhance the cytokine signaling cascade by activating both mitogen-activated protein kinase and NF-κB pathways (52, 53). Aberrant intestinal differentiation may contribute to the initiation of these cascades in Cdx mutants, with inflammation further amplified by upregulation of NLRP3 inflammasome activity. In this regard, we noted that stress-activated mitogen-activated protein kinase pathways were upregulated in *Cdx* mutant intestine (data not shown). Moreover, we found a significant increase in expression of *Nf-κb2*, *Rela*, and the activated form Pser[536]-NF-κB (Fig. 6, *A–C*), whereas *Nf-κb* and *Relb* remained unchanged (Fig. S8, *A* and *B*). Although the basis for these observations is presently unclear, it is tempting to speculate that loss of Cdx function
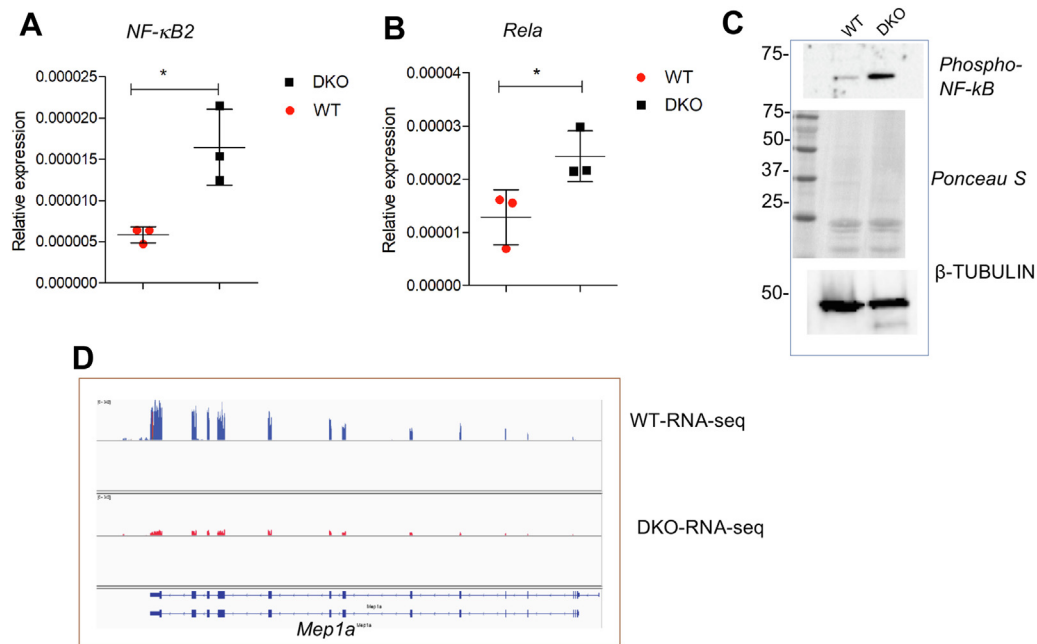
**Figure 6. Cdx impacts *NF-κB* expression.** *A* and *B*, RT–qPCR quantification of relative expression for (*A*) *Nfkb2* and (*B*) *Rela*. *C*, Western blot analysis for phospho-RelA with Ponceau S and β-tubulin as loading controls. *D*, RNA-Seq track at the *Mep1a* locus from WT and DKO colon epithelium. Error bars represent the standard deviation from the mean of three independent biological experiments. Statistical significance was calculated using one-way ANOVA; *$p < 0.05$, ***$p < 0.001$. DKO, double KO; qPCR, quantitative PCR.

contributes to induction of NF-κB signaling, thereby further amplifying TNF-α-mediated inflammatory cascades. Related to this, we also observed downregulation of *MEP1A* in Cdx mutant mice (Fig. 6D) consistent with previous studies suggesting that *MEP1A* is a UC susceptibility gene and is suppressed by TNF-α (24, 54).

### The CDX2–TRIM axis is conserved in UC patients

To determine if CDX status may impact IBD in human populations, we examined publicly accessible RNA-Seq data from UC patients comprised of 24 samples from noninflamed and patient-matched inflamed mucosal tissue. This analysis revealed that *CDX2* was one of the top differentially expressed genes, being reduced in almost all inflamed UC patient samples (Fig. 7A). *TRIM31* levels were also generally reduced in the same samples concomitant with elevation of inflammatory markers, including the NLRP3 product IL-1β (Fig. 7, *B–G*). While these findings are consistent with a conserved CDX–TRIM31–NLRP3 pathway that contributes to IBD pathology, there also appears to be a relative reduction in epithelial cells in samples from inflamed UC patients, as assessed by *EPCAM* expression (Fig. S9), and further analysis will be needed to better establish this relationship.

### Discussion

This study provides evidence for a novel role for Cdx in intestinal inflammation, which has implications for the etiology and therapeutic management of IBD. We demonstrated that *TRIM31* is a novel direct Cdx target gene. *TRIM31* expression was attenuated in Cdx mutant mice concomitant with an increase in the levels of its target, NRLP3, and of

proinflammatory cytokines, including IL-1β, IL-6, IL-18, and TNF-α. Extending these findings, we showed that *CDX2* and *TRIM31* levels were also suppressed in UC patients, concomitant with an increase in *IL-1β* and *TNF-α*, suggesting that this pathway is conserved. We also found that the expression of the NF-κb members *Nf-kb2* and *Rela* were upregulated in Cdx mutant epithelium, suggesting that Cdx loss impacts the expression of these proinflammatory transcription factors through unknown basis.

A number of IBD susceptibility loci have been identified, indicative of complex genetics contributing to the disease (55). Cdx2 has been shown to impact the expression of certain of these genes, prompting us to identify additional Cdx target genes implicated in inflammation. Analysis of genomic distribution of Cdx2 occupancy through ChIP-Seq revealed binding sites that were both gene proximal and intergenic, consistent with Cdx functioning through both distal enhancer motifs as well as proximal regulatory elements, as previously described (21, 36, 56, 57). We also observed that loss of Cdx function impacted chromatin accessibility at a number of putative target genes, including *TRIM31*. This is in agreement with previous findings in both embryonic tissue and the small intestine in which *Cdx2* deletion resulted in a loss of chromatin accessibility for a subset of its targets (21, 47), potentially *via* impact on chromatin remodeling (20, 38, 45, 58).

The persistent production of high levels of proinflammatory cytokines in the gastrointestinal tract is a characteristic of IBD (18). Consistent with a role for Cdx in this process, we found that loss of *Cdx* function was associated with a rapid and pronounced inflammatory response, including induction of IL-1β and TNF-α, among other cytokines and chemokines. We further found that Cdx is a direct regulator of *TRIM31*, which
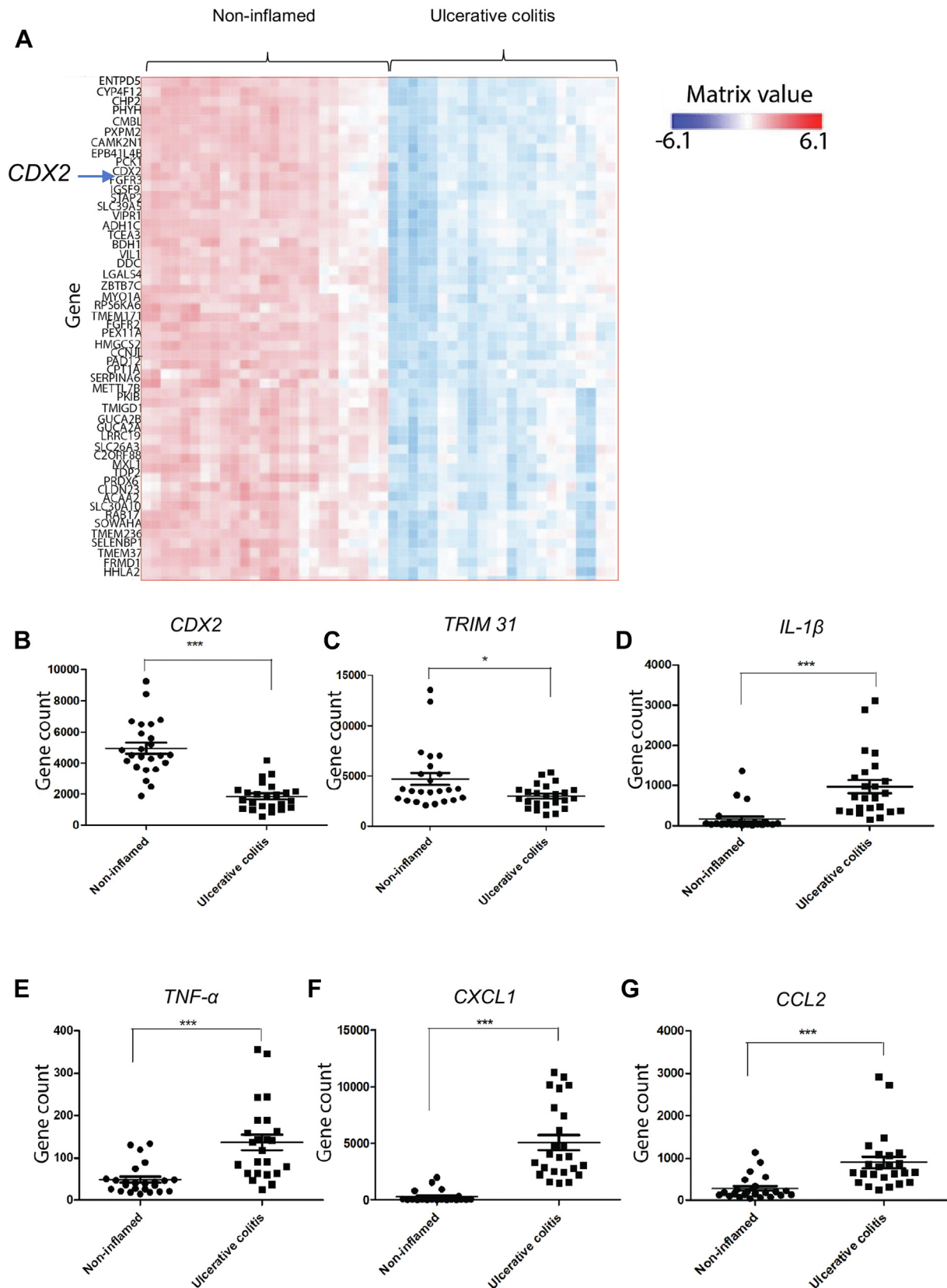
**Figure 7. *CDX2* and *TRIM31* are downregulated in UC patients.** *A*, heatmap for differential gene expression between noninflamed and ulcerative colitis samples from matched patient samples (GSE107597). *B–G*, normalized gene counts for (*B*) *CDX2*; (*C*) *TRIM 31*; (*D*) *IL-1β*; (*E*) *TNF-α*; (*F*) *CXCL1*; and (*G*) *CCL2* from the same samples. Statistical significance was calculated using one-way ANOVA; *p < 0.05, ***p < 0.001. UC, ulcerative colitis.

encodes a negative regulator of the NLRP3 inflammasome (59). Consistent with this, *Cdx* mutants exhibited decreased levels of *TRIM31* concomitant with elevated NLPP3 protein levels and increased inflammasome activity as evidenced by activation of caspase 1 and maturation of its substrate IL-1β. In addition, increased levels of IL-6 were observed in Cdx mutant intestine, in agreement with the known role for IL-1β upstream of the production of this proinflammatory cytokine (60, 61).

Certain other genes encoding proinflammatory effectors, such as *Nfkb2* and *Rela*, also exhibited a gain in chromatin accessibility and concomitant increase in expression in Cdx mutants. While the basis for this is presently unknown, it is possible that the increased TNF-α levels observed in the mutant mice promotes activation of the NF-κB pathway (62, 63). Such activation would provide a mechanistic basis for the induction of expression of NF-κB target genes including those encoding proinflammatory players such as *IL-1β*, *IL-6*, *IL-17*, *Tnfsf13b* as well as chemokines such as *Ccl2* and *Cxcl1*, as also observed in the mutant intestine. In this regard, increased IL-6 protein levels in *Cdx* mutants could be attributed to both NLRP3-dependent IL-1β production, or to induction of NF-κB signaling, another known regulator of IL-6 expression (64–66). In the case of Cdx-dependent intestinal inflammation, a significant amount of IL-6 production would appear to arise from the former, as inhibition of the NLRP3 inflammasome by CY-09 attenuated generation of both IL-1β and IL-6. Irrespective of the source, elevated levels of IL-6 could also contribute to the recruitment of Ly6c-positive monocytes as observed in the Cdx mutants, as IL-6 is required for neutrophil trafficking during the inflammatory response (43, 67). Other chemokines and proinflammatory cytokines, such as *Ccl2* and *Cxcl1*, were also increased in *Cdx* mutants and may also contribute to this chemotaxis.

Treatment with the NLRP3 inhibitor CY-09 reduced the levels of IL-1β and IL-6 and increased the average survival time of Cdx mutants. This finding underscores the pathophysiological consequences of dysregulation of Cdx function specifically upstream of NLRP3 and suggests a potential therapeutic benefit of pharmacological inhibition of NLRP3 in intestinal inflammation. Notably, there was no difference in TNF-α levels between saline-treated and CY-09-treated *Cdx* mutant mice, consistent with TNF-α production independent of NLRP3, the nature of which is presently unknown. TRIM31 is also known to regulate NLRP3 activity *via* ubiquitin-mediated proteasomal degradation, thereby impacting inflammasome assembly (42). In this regard, it is interesting to note that GO analysis identified "proteasome protein catabolic process" as one of the pathways altered in Cdx-DKO mice, suggesting that Cdx may have additional functions related to protein degradation.

A relationship between TNF-α, CDX2, and IBD has been previously suggested. For example, TNFα has been shown to suppress CDX2 expression in model systems, whereas, *in vivo*, anti-TNF-α therapy can restore CDX2 expression levels. In addition, TNF-α suppresses the expression of the CDX2 target gene *MEP1A*, which has also been identified as

an IBD susceptibility locus. Taken together, these findings suggest that TNF-α elicits its inflammatory effects, in part, through attenuation of CDX2 and subsequent impact on downstream targets, at least some of which are implicated in IBD (68, 69). Our present results evoke an additional, novel, mechanism that involves the TRIM–NLRP3–inflammatory pathway wherein loss of Cdx function leads to attenuation of the target gene *TRIM31*, resulting in increased NLRP3 levels and subsequent generation of proinflammatory cytokines. In addition, *in silico* analysis suggests a similar relationship between CDX2 and TRIM31, and inflammation is conserved in UC patients. Taken together, these findings lend support to an important pathogenic role for the CDX2–TRIM31–NLRP3 pathway in IBD and suggest new therapeutic options for the management of chronic intestinal inflammation, which may be particularly germane for patients exhibiting reduction of *CDX2* expression.

## Experimental procedures

### Mouse models and treatment

$Cdx1^{-/-}$-$Cdx2^{fl/fl}$-*Villin*-Cre ER$^T$ mice have been previously described (35, 48, 70). Mice were treated at 12 to 14 weeks of age with a single 4.0 mg dose of tamoxifen to delete *Cdx2*, generating DKO mice. Animals were maintained according to the guidelines of the Canadian Council on Animal Care as approved by the Animal Care and Veterinary Services of the University of Ottawa.

### Cell isolation, organoid culture, and treatment

Colon epithelial cells were enriched by incubating fresh colon tissue in 5 mM EDTA in PBS (pH 8) for 10 min at 4 °C with three to four repeated washes. Each aliquot was collected, and cells run through a 70-μm strainer and either fixed for ChIP-Seq or used to prepare samples for Western blot, RNA-Seq, or ATAC-Seq. In some experiments, filtered cells were incubated with Magnisort beads (Invitrogen; catalog no.: MSNB-6002-74) conjugated to an anti-CD45 antibody (Invitrogen; catalog no.: 13-0451-82) as per the manufacturer's directions. Unbound epithelial cells were recovered and processed for Western blot. Organoid culture from mouse colon was performed as described (71). Organoids were treated with either vehicle (ethanol) or 100 nM 4-hydroxytamoxifen for 72 h to effect deletion of *Cdx2*. Cells were then collected, and RNA was isolated using Trizol.

### ChIP and ChIP-Seq

ChIP and ChIP-Seq were performed as previously described with minor modifications (58, 72, 73). Briefly, colon epithelial cells were isolated as aforementioned, cross-linked with 1% formaldehyde (Sigma; catalog no.: F8775), resuspended in radioimmunoprecipitation buffer, and sonicated to obtain 200- to 500-bp chromatin fragments using a Branson sonicator. Lysates were incubated overnight at 4 °C with primary antibodies or with isotype-specific immunoglobulin G control and DNA recovered and purified. RNA-

Seq library construction and sequencing was conducted by Genome Quebec using an Illumina HiSeq 4000 system. Approximately 25 to 34 M reads were generated for the ChIP-Seq analyses.

### RNA extraction, RNA-Seq, and RT–qPCR

Total RNA was isolated using Trizol or a Qiagen RNeasy mini kit according to the manufacturer's protocol, and RNA quality was assessed by Bioanalyzer. Library construction for and sequencing was performed by Genome Quebec with 19 to 30 M reads per sample. Validation of selected genes from RNA-Seq data was conducted using RT–qPCR on a CFX96 Bio-Rad thermocycler with Go-Taq SYBR Green master mix (Promega). Analyses were performed based on the Ct values from the target gene and internal control gene (18s rRNA). All primers for PCR analyses are noted in Table S1.

### ATAC-Seq analysis

Colon cells were collected as aforementioned and treated for 30 to 40 min at 37 °C with trypsin to obtain single-cell suspensions. Approximately 100,000 cells were used for the transposase reaction as previously described (74). Briefly, cells were resuspended in cold lysis buffer (10 mM Tris–Cl at pH 7.4, 10 mM NaCl, 3 mM MgCl$_2$, and 0.1% Igepal CA-360), and crude nuclear pellets were incubated in transposition mix for 20 to 30 min at 37 °C. DNA was then purified using the MinElute PCR purification kit (Qiagen), PCR amplified using NEBNext High-Fidelity master mix, a common forward primer, and uniquely barcoded reverse primers for each sample. The reaction was purified using MinElute PCR purification kits (Qiagen), and primer dimers were removed using Ampure XP beads (Beckman Coulter). Library construction and paired-end sequencing were performed using an Illumina Hi-Seq 4000 system by Genome Quebec and sequenced to a depth of 55 to 72 M reads.

### Western blot and ELISA

Whole-cell lysates were prepared from colon epithelial cells, proteins resolved by SDS-polyacrylamide gel electrophoresis, and then transferred onto nitrocellulose membranes for immunoblot analysis. Primary antibodies used were anti-Cdx2 at 1:1000 dilution (19), anti–caspase-1 (Thermo Fisher Scientific), anti-NLRP3 (Thermo Fisher Scientific), anti–β-tubulin (Santa Cruz), anti–phospho-ser$^{536}$NF-κB (Cell Signalling), anti–Il-1β, and anti–β-actin (Santa Cruz). ELISA was conducted on colon epithelial lysates using kits from BD Bioscience as recommended by the supplier.

### IF

Colon tissue was dissected, fixed in 4% paraformaldehyde at 4 °C overnight, and then transferred to 70% ethanol. Tissue was embedded in paraffin, and 4 μm sections were mounted on slides. Paraffin-embedded tissue sections were deparaffinized in xylene and rehydrated in an ethanol series. Antigen retrieval was carried out using a Decloaking chamber with immersion in citrate buffer (10 mM citric acid, 0.05% Tween-20, pH 6.0). Slides were allowed to cool down while in citrate buffer for 30 min at room temperature, then washed in water for 5 min. Sections were incubated in a blocking solution (5% goat serum, 4% bovine serum albumin, 10% sucrose in 1× Tris-buffered saline [TBS]) for 1 h at room temperature in a humidified chamber and then incubated with anti-NLRP3 primary antibody (Invitrogen; catalog no.: MA5-32255) at a 1:500 dilution in antibody diluent (1% bovine serum albumin, 10% sucrose in 1× TBS) at 4 °C overnight in a humidified chamber followed by three 5-min washes in 1× TBS. Negative control sections were incubated in antibody diluent instead of primary antibody. Sections were then incubated with goat anti-rabbit Alexa-Fluor 488 secondary antibody (Invitrogen; catalog no.: A-11008) for 1 h at room temperature in a dark humidified chamber, washed three times for 5 min each in 1× TBS, and mounted with Fluorescence Mounting Medium (Dako Omnis; code S3023). Images were captured using a Zeiss AxioImager M2.

### Flow cytometry

Cells were washed twice in 2 ml of cold PBS for 5 min, fixed in 4% paraformaldehyde for 20 min at room temperature, pretreated with anti-Fc antibody for 1 h and subsequently for 2 h with fluorophore-conjugated antibodies (EPCAM BioLegend, catalog no.: 118215; CD45 BioLegend, catalog no.: 147711; Ly6C BioLegend, catalog no.: 128015, or Ly6G BioLegend, catalog no.: 127625). Cells were then washed to remove excess antibody, and dead/live staining was performed using zombie yellow (BioLegend) as per the manufacturer's directions and assessed using a BD LSFRFortessa.

### In vivo NLRP3 inhibition

Mice (12–14 weeks old) were treated with either the NLRP3 inhibitor CY-09 (2.5 mg/kg; MilliporeSigma) or saline, following which animals were treated with tamoxifen or vehicle on day 2 and treatment with CY-09 or saline continued to day 6 post-tamoxifen or until the animals became moribund.

### Heterologous promoter analysis

The *TRIM31* promoter region (1176 bp upstream of the start codon) containing either a WT (TTTATG) or mutated (CCATGG) CDRE was cloned into the PxP2 luciferase reporter vector. C2BBE1 cells, cultured under standard conditions, were transfected in triplicate using Lipofectamine and 1 μg of the appropriate luciferase reporter construct, 1 μg of *Cdx2* expression vector (or empty vector control), 0.2 μg of an *xgal* expression vector, and 100 ng of *GFP* expression vector to a total of 2.3 μg of DNA per transfection. Cells were harvested 48 h post-transfection, and lysates were analyzed using the Promega Luciferase Assay System, using β-galactosidase activity to correct for transfection efficiency as described previously (70).

### Bioinformatics analyses

Bioconductor coupled with R-packages and Partek Flow (Partec, Inc) was used as follows.

### RNA-Seq data analysis

Expression of transcripts was quantified with Salmon (version 1.3.0) (75) against an index built from the GENCODE vM25 assembly with the inclusion of genomic decoy sequences. Data were loaded into R using the tximport library (76), and the gene/count matrix was filtered to retain only genes with five or more mapped reads in two or more samples. Differential expression was assessed using DESeq2, version 1.30 (77). Expression differences between DKO *versus* WT replicates were calculated using the DESeq2 lfcShrink function, applying the apeglm method (78). Multiple testing correction was performed using the Benjamini–Hochberg method, and lists of significantly differentially expressed genes were identified using a $q$ value (*i.e.*, a corrected $p$ value) cutoff of 0.05.

ClusterProfiler (79) was used to perform functional enrichment analysis to find classes that are enriched in genes that were differentially expressed in Cdx DKO mutants relative to controls. Using ClusterProfiler, we performed hypergeometric tests to identify GO Biological Processes, Molecular Function terms, and Kyoto Encyclopedia of Genes and Genomes pathways that were overrepresented in these differentially expressed genes, analyzing each annotation set and each direction of differential expression independently.

### Genome enrichment patterns

ChIP-Seq and ATAC-Seq reads were aligned to the mm10 genome sequence using bwa, version 0.7.10 (80). The resulting BAM files were converted to bigwig format using deepTools2 (81) bamCoverage, scaling the signal to counts per million. Protein coding gene TSSs were extracted from Encode, v101 database using BioMart. DeepTools computeMatrix was used to calculate the coverage of Cdx2, H3K4me3 ChIP-Seq, and ATAC-Seq reads in the region around each TSS. plotHeatmap was then used to plot the coverage patterns for all factors, separating TSSs into genes significantly up, down, or with no significant fold change in mutants relative to controls.

### Statistical analyses

Statistical analyses were performed using Microsoft Excel and GraphPad Prism 8.0 (GraphPad Software, Inc). Statistical significance was calculated using $t$ test and one-way ANOVA; *$p < 0.05$, **$p < 0.01$, ***$p < 0.001$, or ****$p < 0.0001$.

### Data availability

RNA-Seq data presented in this article have been deposited at Gene Expression Omnibus (NCBI) with the study accession codes; GSE and GSE. ChIP-Seq and ATAC-Seq data were deposited with the study accession codes (to be provided). IBD patient data were obtained from Gene Expression Omnibus accession number GSE107597.

### References

1. Baumgart, D. C., and Sandborn, W. J. (2007) Inflammatory bowel disease: clinical aspects and established and evolving therapies. *Lancet (London, England)* **369**, 1641–1657
2. Hazel, K., and O'Connor, A. (2020) Emerging treatments for inflammatory bowel disease. *Ther. Adv. Chronic Dis.* **11**. https://doi.org/10.1177/2040622319899297
3. Baumgart, D. C., and Carding, S. R. (2007) Inflammatory bowel disease: cause and immunobiology. *Lancet (London, England)* **369**, 1627–1640
4. Watts, D. A., and Satsangi, J. (2002) The genetic jigsaw of inflammatory bowel disease. *Gut* **50**, iii31
5. Graham, D. B., and Xavier, R. J. (2020) Pathway paradigms revealed from the genetics of inflammatory bowel disease. *Nature* **578**, 527–539
6. Ellinghaus, D., Jostins, L., Spain, S. L., Cortes, A., Bethune, J., Han, B., *et al*. (2016) Analysis of five chronic inflammatory diseases identifies 27 new associations and highlights disease-specific patterns at shared loci. *Nat. Genet.* **48**, 510–518
7. Khatri, V., and Kalyanasundaram, R. (2021) Therapeutic implications of inflammasome in inflammatory bowel disease. *FASEB J.* **35**, e21439
8. Zaki, M. H., Lamkanfi, M., and Kanneganti, T. D. (2011) The Nlrp3 inflammasome: Contributions to intestinal homeostasis. *Trends Immunol.* **32**, 171–179
9. Guo, H., Callaway, J. B., and Ting, J. P. Y. (2015) Inflammasomes: mechanism of action, role in disease, and therapeutics. *Nat. Med.* **21**, 677–687
10. Swanson, K. V., Deng, M., and Ting, J. P. Y. (2019) The NLRP3 inflammasome: molecular activation and regulation to therapeutics. *Nat. Rev. Immunol.* **19**, 477–489
11. Tourkochristou, E., Aggeletopoulou, I., Konstantakis, C., and Triantos, C. (2019) Role of NLRP3 inflammasome in inflammatory bowel diseases. *World J. Gastroenterol.* **25**, 4796–4804

12. Zhen, Y., and Zhang, H. (2019) NLRP3 inflammasome and inflammatory bowel disease. *Front. Immunol.* **10**, 276

13. Chen, Q. L., Yin, H. R., He, Q. Y., and Wang, Y. (2021) Targeting the NLRP3 inflammasome as new therapeutic avenue for inflammatory bowel disease. *Biomed. Pharmacother.* **138**, 111442

14. Shao, B. Z., Wang, S. L., Pan, P., Yao, J., Wu, K., Li, Z. S., *et al.* (2019) Targeting NLRP3 inflammasome in inflammatory bowel disease: putting out the fire of inflammation. *Inflammation* **42**, 1147–1159

15. Schroder, K., and Tschopp, J. (2010) The inflammasomes. *Cell* **140**, 821–832

16. Latz, E., Xiao, T. S., and Stutz, A. (2013) Activation and regulation of the inflammasomes. *Nat. Rev. Immunol.* **13**, 397–411

17. Garrett, W. S., Gordon, J. I., and Glimcher, L. H. (2010) Homeostasis and inflammation in the intestine. *Cell* **140**, 859–870

18. Coskun, M., Troelsen, J. T., and Nielsen, O. H. (2011) The role of CDX2 in intestinal homeostasis and inflammation. *Biochim. Biophys. Acta* **1812**, 283–289

19. Savory, J. G., Pilon, N., Grainger, S., Sylvestre, J. R., Béland, M., Houle, M., *et al.* (2009) Cdx1 and Cdx2 are functionally equivalent in vertebral patterning. *Dev. Biol.* **330**, 114–122

20. Nguyen, T. T., Savory, J. G., Brooke-Bisschop, T., Ringuette, R., Foley, T., Hess, B. L., *et al.* (2017) Cdx2 regulates gene expression through recruitment of Brg1-associated switch-sucrose non-fermentable (SWI-SNF) chromatin remodeling activity. *J. Biol. Chem.* **292**, 3389–3399

21. Verzi, M. P., Shin, H., San Roman, A. K., Liu, X. S., and Shivdasani, R. A. (2013) Intestinal master transcription factor CDX2 controls chromatin access for partner transcription factor binding. *Mol. Cell Biol.* **33**, 281–292

22. Coskun, M. (2014) The role of CDX2 in inflammatory bowel disease. *Dan Med. J.* **61**, B4820

23. Coskun, M., Olsen, A. K., Bzorek, M., Holck, S., Engel, U. H., Nielsen, O. H., *et al.* (2014) Involvement of CDX2 in the cross talk between TNF-α and Wnt signaling pathway in the colon cancer cell line Caco-2. *Carcinogenesis* **35**, 1185–1192

24. Coskun, M., Olsen, A. K., Holm, T. L., Kvist, P. H., Nielsen, O. H., Riis, L. B., *et al.* (2012) TNF-α-induced down-regulation of CDX2 suppresses MEP1A expression in colitis. *Biochim. Biophys. Acta* **1822**, 843–851

25. Coskun, M., Soendergaard, C., Joergensen, S., Dahlgaard, K., Riis, L. B., Nielsen, O. H., *et al.* (2017) Regulation of laminin γ2 expression by CDX2 in colonic epithelial cells is impaired during active inflammation. *J. Cell Biochem.* **118**, 298–307

26. Boyd, M., Hansen, M., Jensen, T. G., Perearnau, A., Olsen, A. K., Bram, L. L., *et al.* (2010) Genome-wide analysis of CDX2 binding in intestinal epithelial cells (Caco-2). *J. Biol. Chem.* **285**, 25115–25125

27. Koslowski, M. J., Kübler, I., Chamaillard, M., Schaeffeler, E., Reinisch, W., Wang, G., *et al.* (2009) Genetic variants of Wnt transcription factor TCF-4 (TCF7L2) putative promoter region are associated with small intestinal Crohn's disease. *PLoS One* **4**, e4496

28. Morosi, L. G., Cutine, A. M., Cagnoni, A. J., Manselle-Cocco, M. N., Croci, D. O., Merlo, J. P., *et al.* (2021) Control of intestinal inflammation by glycosylation-dependent lectin-driven immunoregulatory circuits. *Sci. Adv.* **7**, eabf8630

29. Saiz, M. L., Cibrian, D., Ramírez-Huesca, M., Torralba, D., Moreno-Gonzalo, O., and Sánchez-Madrid, F. (2017) Tetraspanin CD9 limits mucosal healing in experimental colitis. *Front. Immunol.* **8**, 1854

30. Calon, A., Gross, I., Lhermitte, B., Martin, E., Beck, F., Duclos, B., *et al.* (2007) Different effects of the Cdx1 and Cdx2 homeobox genes in a murine model of intestinal inflammation. *Gut* **56**, 1688–1695

31. Tsuchiya, K., Hayashi, R., Fukushima, K., Hibiya, S., Horita, N., Negi, M., *et al.* (2017) Caudal type homeobox 2 expression induced by leukocytapheresis might be associated with mucosal healing in ulcerative colitis. *J. Gastroenterol. Hepatol.* **32**, 1032–1039

32. Davidson, A. J., and Zon, L. I. (2006) The caudal-related homeobox genes cdx1a and cdx4 act redundantly to regulate hox gene expression and the formation of putative hematopoietic stem cells during zebrafish embryogenesis. *Dev. Biol.* **292**, 506–518

33. van den Akker, E., Forlani, S., Chawengsaksophak, K., de Graaff, W., Beck, F., Meyer, B. I., *et al.* (2002) Cdx1 and Cdx2 have overlapping functions in anteroposterior patterning and posterior axis elongation. *Development* **129**, 2181–2193

34. Chawengsaksophak, K., James, R., Hammond, V. E., Köntgen, F., and Beck, F. (1997) Homeosis and intestinal tumours in Cdx2 mutant mice. *Nature* **386**, 84–87

35. Hryniuk, A., Grainger, S., Savory, J. G., and Lohnes, D. (2012) Cdx function is required for maintenance of intestinal identity in the adult. *Dev. Biol.* **363**, 426–437

36. Grainger, S., Savory, J. G., and Lohnes, D. (2010) Cdx2 regulates patterning of the intestinal epithelium. *Dev. Biol.* **339**, 155–165

37. Kumar, N., Tsai, Y. H., Chen, L., Zhou, A., Banerjee, K. K., Saxena, M., *et al.* (2019) The lineage-specific transcription factor CDX2 navigates dynamic chromatin to control distinct stages of intestine development. *Development* **146**, dev172189

38. Bonhomme, C., Duluc, I., Martin, E., Chawengsaksophak, K., Chenard, M. P., Kedinger, M., *et al.* (2003) The Cdx2 homeobox gene has a tumour suppressor function in the distal colon in addition to a homeotic role during gut development. *Gut* **52**, 1465–1471

39. San Roman, A. K., Tovaglieri, A., Breault, D. T., and Shivdasani, R. A. (2015) Distinct processes and transcriptional targets underlie CDX2 requirements in intestinal stem cells and differentiated villus cells. *Stem Cell Rep.* **5**, 673–681

40. Hryniuk, A., Grainger, S., Savory, J. G., and Lohnes, D. (2014) Cdx1 and Cdx2 function as tumor suppressors. *J. Biol. Chem.* **289**, 33343–33354

41. Ra, E. A., Lee, T. A., Won Kim, S., Park, A., Choi, H. J., Jang, I., *et al.* (2016) TRIM31 promotes Atg5/Atg7-independent autophagy in intestinal cells. *Nat. Commun.* **7**, 11726

42. Song, H., Liu, B., Huai, W., Yu, Z., Wang, W., Zhao, J., *et al.* (2016) The E3 ubiquitin ligase TRIM31 attenuates NLRP3 inflammasome activation by promoting proteasomal degradation of NLRP3. *Nat. Commun.* **7**, 13727

43. McGeough, M. D., Pena, C. A., Mueller, J. L., Pociask, D. A., Broderick, L., Hoffman, H. M., *et al.* (2012) Cutting edge: IL-6 is a marker of inflammation with no direct role in inflammasome-mediated mouse models. *J. Immunol.* **189**, 2707–2711

44. Foley, T. E., Hess, B., Savory, J. G. A., Ringuette, R., and Lohnes, D. (2019) Role of Cdx factors in early mesodermal fate decisions. *Development* **146**, dev170498

45. Amin, S., Neijts, R., Simmini, S., van Rooijen, C., Tan, S. C., Kester, L., *et al.* (2016) Cdx and T Brachyury Co-activate growth signaling in the embryonic axial progenitor niche. *Cell Rep.* **17**, 3165–3177

46. Huang, D., Guo, G., Yuan, P., Ralston, A., Sun, L., Huss, M., *et al.* (2017) The role of Cdx2 as a lineage specific transcriptional repressor for pluripotent network during the first developmental cell lineage segregation. *Sci. Rep.* **7**, 17156

47. Suh, E., Chen, L., Taylor, J., and Traber, P. G. (1994) A homeodomain protein related to caudal regulates intestine-specific gene transcription. *Mol. Cell Biol.* **14**, 7340–7351

48. Subramanian, V., Meyer, B. I., and Gruss, P. (1995) Disruption of the murine homeobox gene Cdx1 affects axial skeletal identities by altering the mesodermal expression domains of Hox genes. *Cell* **83**, 641–653

49. Maier, E. A., Dusing, M. R., and Wiginton, D. A. (2005) Cdx binding determines the timing of enhancer activation in postnatal duodenum. *J. Biol. Chem.* **280**, 13195–13202

50. Taylor, J. K., Levy, T., Suh, E. R., and Traber, P. G. (1997) Activation of enhancer elements by the homeobox gene Cdx2 is cell line specific. *Nucl. Acids Res.* **25**, 2293–2300

51. Jiang, H., He, H., Chen, Y., Huang, W., Cheng, J., Ye, J., *et al.* (2017) Identification of a selective and direct NLRP3 inhibitor to treat inflammatory disorders. *J. Exp. Med.* **214**, 3219–3238

52. Meldrum, D. R. (1998) Tumor necrosis factor in the heart. *Am. J. Physiol.* **274**, R577–R595

53. Wright, G., Singh, I. S., Hasday, J. D., Farrance, I. K., Hall, G., Cross, A. S., *et al.* (2002) Endotoxin stress-response in cardiomyocytes: NF-kappaB activation and tumor necrosis factor-alpha expression. *Am. J. Physiol. Heart Circ. Physiol.* **282**, H872–H879

54. Banerjee, S., Oneda, B., Yap, L. M., Jewell, D. P., Matters, G. L., Fitzpatrick, L. R., *et al.* (2009) MEP1A allele for meprin A metalloprotease is a

susceptibility gene for inflammatory bowel disease. *Mucosal Immunol.* **2**, 220–231

55. Xavier, R. J., and Podolsky, D. K. (2007) Unravelling the pathogenesis of inflammatory bowel disease. *Nature* **448**, 427–434

56. Verzi, M. P., Hatzis, P., Sulahian, R., Philips, J., Schuijers, J., Shin, H., *et al.* (2010) TCF4 and CDX2, major transcription factors for intestinal function, converge on the same cis-regulatory regions. *Proc. Natl. Acad. Sci. U. S. A.* **107**, 15157–15162

57. Savory, J. G., Bouchard, N., Pierre, V., Rijli, F. M., De Repentigny, Y., Kothary, R., *et al.* (2009) Cdx2 regulation of posterior development through non-Hox targets. *Development* **136**, 4099–4110

58. Saxena, M., Roman, A. K. S., O'Neill, N. K., Sulahian, R., Jadhav, U., and Shivdasani, R. A. (2017) Transcription factor-dependent 'anti-repressive' mammalian enhancers exclude H3K27me3 from extended genomic domains. *Genes Dev.* **31**, 2391–2404

59. Poudel, B., and Gurung, P. (2018) An update on cell intrinsic negative regulators of the NLRP3 inflammasome. *J. Leukoc. Biol.* **103**, 1165–1177

60. Tanaka, T., and Kishimoto, T. (2014) The biology and medical implications of interleukin-6. *Cancer Immunol. Res.* **2**, 288–294

61. Tanaka, T., Narazaki, M., and Kishimoto, T. (2014) IL-6 in inflammation, immunity, and disease. *Cold Spring Harb. Perspect. Biol.* **6**, a016295

62. Gupta, S. C., Sundaram, C., Reuter, S., and Aggarwal, B. B. (2010) Inhibiting NF-κB activation by small molecules as a therapeutic strategy. *Biochim. Biophys. Acta* **1799**, 775–787

63. Liu, T., Zhang, L., Joo, D., and Sun, S.-C. (2017) NF-κB signaling in inflammation. *Signal. Transduct. Target. Ther.* **2**, 17023

64. Libermann, T. A., and Baltimore, D. (1990) Activation of interleukin-6 gene expression through the NF-kappa B transcription factor. *Mol. Cell. Biol.* **10**, 2327–2334

65. Tak, P. P., and Firestein, G. S. (2001) NF-kappaB: a key role in inflammatory diseases. *J. Clin. Invest.* **107**, 7–11

66. De Cesaris, P., Starace, D., Riccioli, A., Padula, F., Filippini, A., and Ziparo, E. (1998) Tumor necrosis factor-alpha induces interleukin-6 production and integrin ligand expression by distinct transduction pathways. *J. Biol. Chem.* **273**, 7566–7571

67. Fielding, C. A., McLoughlin, R. M., McLeod, L., Colmont, C. S., Najdovska, M., Grail, D., *et al.* (2008) IL-6 regulates neutrophil trafficking during acute inflammation *via* STAT3. *J. Immunol.* **181**, 2189–2195

68. Lichtenstein, G. R. (2013) Comprehensive review: antitumor necrosis factor agents in inflammatory bowel disease and factors implicated in treatment response. *Therap. Adv. Gastroenterol.* **6**, 269–293

69. Nielsen, O. H., and Ainsworth, M. A. (2013) Tumor necrosis factor inhibitors for inflammatory bowel disease. *New Engl. J. Med.* **369**, 754–762

70. Su, L. K., Kinzler, K. W., Vogelstein, B., Preisinger, A. C., Moser, A. R., Luongo, C., *et al.* (1992) Multiple intestinal neoplasia caused by a mutation in the murine homolog of the APC gene. *Science* **256**, 668–670

71. O'Rourke, K. P., Ackerman, S., Dow, L. E., and Lowe, S. W. (2016) Isolation, culture, and maintenance of mouse intestinal stem cells. *Bio Protoc.* **6**, e1733

72. Jahan, S., Xu, W., He, S., Gonzalez, C., Delcuve, G. P., and Davie, J. R. (2016) The chicken erythrocyte epigenome. *Epigenetics Chromatin* **9**, 19

73. Jahan, S., Beacon, T. H., Xu, W., and Davie, J. R. (2020) Atypical chromatin structure of immune-related genes expressed in chicken erythrocytes. *Biochem. Cell Biol.* **98**, 171–177

74. Buenrostro, J. D., Giresi, P. G., Zaba, L. C., Chang, H. Y., and Greenleaf, W. J. (2013) Transposition of native chromatin for fast and sensitive epigenomic profiling of open chromatin, DNA-binding proteins and nucleosome position. *Nat. Met.* **10**, 1213–1218

75. Patro, R., Duggal, G., Love, M. I., Irizarry, R. A., and Kingsford, C. (2017) Salmon provides fast and bias-aware quantification of transcript expression. *Nat. Met.* **14**, 417–419

76. Soneson, C., Love, M. I., and Robinson, M. D. (2015) Differential analyses for RNA-seq: transcript-level estimates improve gene-level inferences. *F1000Research* **4**, 1521

77. Love, M. I., Huber, W., and Anders, S. (2014) Moderated estimation of fold change and dispersion for RNA-seq data with DESeq2. *Genome Biol.* **15**, 550

78. Zhu, A., Ibrahim, J. G., and Love, M. I. (2019) Heavy-tailed prior distributions for sequence count data: removing the noise and preserving large differences. *Bioinformatics* **35**, 2084–2092

79. Yu, G., Wang, L. G., Han, Y., and He, Q. Y. (2012) clusterProfiler: an R package for comparing biological themes among gene clusters. *OMICS* **16**, 284–287

80. Li, H. (2013) Aligning sequence reads, clone sequences and assembly contigs with BWA-MEM. *ArXiv.* https://doi.org/10.48550/arXiv.1303.3997

81. Ramírez, F., Ryan, D. P., Grüning, B., Bhardwaj, V., Kilpert, F., Richter, A. S., *et al.* (2016) deepTools2: a next generation web server for deep-sequencing data analysis. *Nucl. Acids Res.* **44**, W160–W165